

Research Article

Toughness Enhancement of PLA-Based Filaments for Material Extrusion 3D Printing

Siriwan Pongsathit,¹ Jutamas Kamaisoom,¹ Atikarn Rungteerabandit,¹ Pakorn Opaprakasit,² Krit Jiamjiroch,³ and Cattaleeya Pattamaprom ¹

¹Research Unit in Polymer Rheology and Processing, Department of Chemical Engineering, Faculty of Engineering, Thammasat University, Pathumthani 12120, Thailand

²School of Integrated Science and Innovation, Sririndhorn International Institute of Technology, Thammasat University, Pathumthani 12120, Thailand

³Department of Mechanical Engineering, Faculty of Engineering, Thammasat University, Pathumthani 12120, Thailand

Correspondence should be addressed to Cattaleeya Pattamaprom; cattalee@engr.tu.ac.th

Received 16 April 2023; Revised 12 July 2023; Accepted 29 July 2023; Published 9 August 2023

Academic Editor: Enrico Salvati

Copyright © 2023 Siriwan Pongsathit et al. This is an open access article distributed under the Creative Commons Attribution License, which permits unrestricted use, distribution, and reproduction in any medium, provided the original work is properly cited.

Poly(lactic acid) (PLA) is one of the most popular biodegradable thermoplastics in the market of 3D printing filaments used in the material extrusion (ME) technique. This is because it can be printed easily at low temperatures. However, its inherent brittleness limits its use in many applications. In this work, the toughness of PLA filament was improved by blending with various types of rubbers including natural rubber (NR), acrylic core-shell rubber (CSR), and thermoplastic polyurethane (TPU) in the amount of 15% by weight. PLA/TPU filament was found to have the smoothest surface with the best shape and dimension stability, while PLA/NR filament rendered the highest tensile toughness. In term of the effect of printing temperature, the highest printing temperature in this study (210°C) provided the highest smoothness with the best shape stability and dimension accuracy. Interestingly, the tensile toughness and elongation at break of 3D printed specimens were found to be higher than those of compression-molded specimens for all filament types. This could be explained by the ability of the 3D printing technique to produce specimens that aligned in the printing direction in a fiber-like pattern.


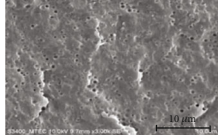

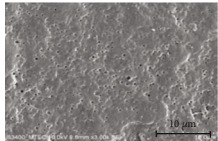
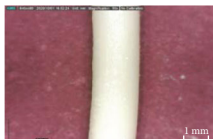
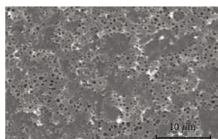

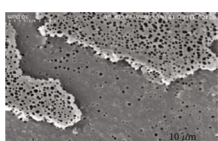

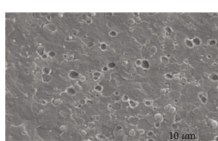

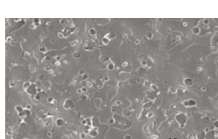

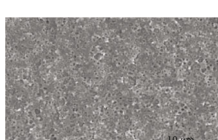


1. Introduction

Additive manufacturing, also known as 3D printing, has become a very interesting forming process as it possesses the ability to fabricate customized objects with complex designs at a small production cost [1, 2]. Furthermore, it could minimize material waste potentially making the production more sustainable [3, 4]. Material extrusion (ME) is the most widely used 3D printing technique due to its low machine and material costs. This technique creates products by extruding a molten thermoplastic filament layer by layer through a nozzle [5]. So far, 3D printing has been employed in the preproduction, prototyping, and postfabrication phases. In the automotive and aerospace industries, the use of 3D-printed components as part of the design process is

commonplace. This is because new designs can be generated without needs of new molds or complex tooling.

Nowadays, many polymers has been investigated as 3D printing filaments, such as acrylonitrile butadiene styrene (ABS) [6, 7], polycarbonate (PC) [8], polyetherimide (PEI) [9], polyamide (PA) [10], polylactic acid (PLA) [11, 12], and high- and low-density polyethylene (HDPE and LDPE) [13]. However, the most popular commodity thermoplastic filaments used in ME 3D printers are PLA and ABS [14, 15]. The advantages of PLA filaments are lower printing temperature, minimal warpage, and good optical transparency. Furthermore, PLA is a cheaper thermoplastic filament with excellent biocompatibility and biodegradability [16, 17]. Nevertheless, its inherent brittleness limits the use of 3D-printed PLA specimens as demoprototypes rather than

TABLE 1: The filament diameters and morphologies of all PLA/rubber filaments taken by a digital microscope at 50x magnification and by SEM at 3000x magnification.

| Screw speed (rpm) | Filament diameter \pm S.D (mm) | Morphologies | |
|--------------------|----------------------------------|--|---|
| | | Surface of filaments (50x) | Cross-section of filaments (3000x) |
| (a) PLA/NR | | | |
| 50 | 1.60 \pm 0.05 mm |  |  |
| 70 | 1.67 \pm 0.13 mm |  |  |
| 80 | 1.70 \pm 0.12 mm |  |  |
| 90 | 1.80 \pm 0.12 mm |  |  |
| (b) PLA/TPU | | | |
| 60 | 1.67 \pm 0.05 mm |  |  |
| 70 | 1.81 \pm 0.06 mm |  |  |
| (c) PLA/CSR | | | |
| 60 | 1.52 \pm 0.05 mm |  |  |
| 70 | 1.82 \pm 0.06 mm |  |  |

actual products in most cases [18]. Recently, PLA modified by blending with other polymers and additives has been investigated as filaments for 3D printers [19–27]. Ou-Yang et al. [24] studied the blends of poly(butylene succinate) (PBS) and PLA as filaments for 3D printers and found that

the higher PBS content led to higher elongation at break and impact strength, where the PBS/PLA ratios of 60/40 and 40/60 could provide good dimensional accuracy and gloss. Prasong et al. [25] found that the blends of 30 wt% poly(butylene adipate-co-terephthalate) (PBAT) in PLA

could enhance the elongation at break of 3D-printed specimens by 26 times compared to PLA specimens. On the other hand, the research on using rubbers to improve the toughness of PLA filaments remains limited. So far, only two reports have been published: one used acrylic core-shell rubber (CSR) [26] and the other used natural rubber (NR) [27] as toughening agents for PLA filaments. In their work, the 3D-printed PLA/CSR specimens exhibited lower mechanical properties than those of 3D-printed PLA specimen [26]. For PLA/NR filaments, the elongation at break and impact strength of the PLA/NR 3D-printed specimens at NR content of up to 20 wt% were found to increase with increasing rubber content. However, the fluctuation in the diameters of PLA/NR filaments in this work resulted in undesirable porosities of the fabricated samples. Previously, our research group investigated the toughness improvement of PLA by blending with various rubbers and found that CSR and masticated NR could provide significantly higher impact strength and tensile toughness to compression-molded PLA samples. We also discovered that among all PLA/rubber blends, thermoplastic polyurethane (TPU) could provide the highest tensile strength [28, 29].

Therefore, the blends of PLA with CSR, NR, and TPU were investigated in this work for their potential as 3D printing filaments with enhanced toughness. The extrusion conditions used in producing filaments from these compounds were studied for their effect on the filament diameter and size consistency. Moreover, the effect of printing temperature was also investigated on various properties of 3D-printed specimens including the morphological, thermal, and mechanical properties and shape stability. The prepared 3D-printed specimens could be potentially used in the applications that require higher material toughness such as bumpers, cushioning materials, seals, helmets, or bicycle frames.

2. Experimental

2.1. Materials. Poly(lactic acid) or PLA grade 4043D was produced by NatureWorks LLC. Acrylic core-shell rubber (CSR) was manufactured by Dow Chemicals Company with the trade name Paraloid™ BPM-520. The thermoplastic polyurethane (TPU) grade WHT-11951C was purchased from Able One Engineering Co., Ltd. (Thailand). Natural rubber (NR) grade STR5L was obtained from Natural Art and Technology Co., Ltd. (Thailand). The grade of commercial PLA filaments used in this study was the transparent grade produced by SUNLU.

2.2. Raw Material Preparation

2.2.1. Preparation of Natural Rubber Masterbatch. Due to the high molecular weight of NR, a masterbatch of NR/PLA was prepared at a 50:50 ratio to facilitate the dispersion of NR in the PLA matrix. The masterbatch was prepared in a Banbury-type internal mixer (YF-SBI-3L, Yong Fong Machinery Co., Ltd., Thailand) at 150°C with a rotor speed of 60 rpm. The NR was first masticated for 3 min before adding PLA and other additives. Then, the compounding was continued until the mixing time reached 15 min.

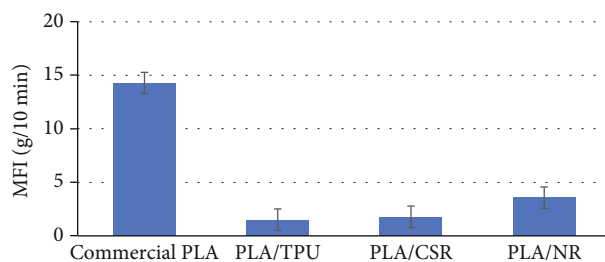


FIGURE 1: Melt flow indexes of commercial PLA and PLA/rubber blends measured at 190°C.

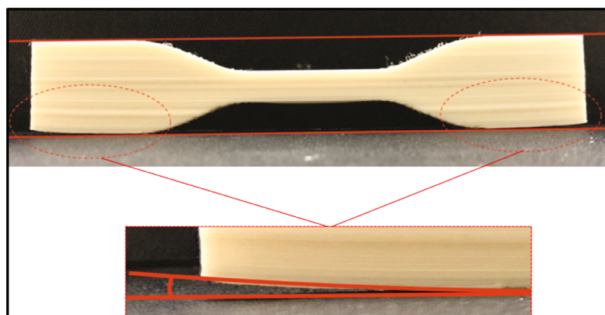


FIGURE 2: The measurement of warpage angle of 3D-printed dumbbell-shaped specimens.

2.2.2. Preparation of PLA/Rubber Blends. The rubber (NR/PLA masterbatch, CSR, or TPU) was blended with PLA in an internal mixer (Brabender® Plasticorder 350E 3Z) at 160°C at a rotor speed of 60 rpm for 12 min. The rubber content in the compound was fixed at 15 wt%. PLA, NR/PLA masterbatch, TPU, and CSR were dried to remove moisture before compounding. The compounds obtained were ground into small pellets with a plastic granulator (ZERMA Co., Ltd., Thailand).

2.2.3. Preparation of 3D Printing Filaments. In this research, filaments were fabricated by using a twin-screw plastic extruder (Labtech Engineering Co., Ltd., Thailand) with an L/D ratio of 40, a screw diameter of 16 mm, and a die diameter of 1.75 mm. The temperature profiles in the barrel were set at 160°C–190°C from the feeding hopper to the die head. To obtain the appropriate filament diameter in the range of 1.7–1.9 mm, the screw speeds were varied from 40 to 90 rpm, while the nip roll speed was fixed at 3 m/min.

2.2.4. Specimen Preparation. In this work, the PLA/rubber specimens were prepared using two methods: conventional compression molding and ME 3D printing.

(1) Preparation of Compression-Molded Specimens. In this study, the compression-molded specimens were prepared as a reference for comparison. The dried PLA and PLA/rubber blends were compressed into sheets at 190°C and a pressure of 1500 psi for 20 min. Then, the compressed sheets were then cut into dumbbell-shaped specimens according to the ASTM D368 type IV standard by laser cutting. The mechanical properties of at least five specimens were measured for each formulation.

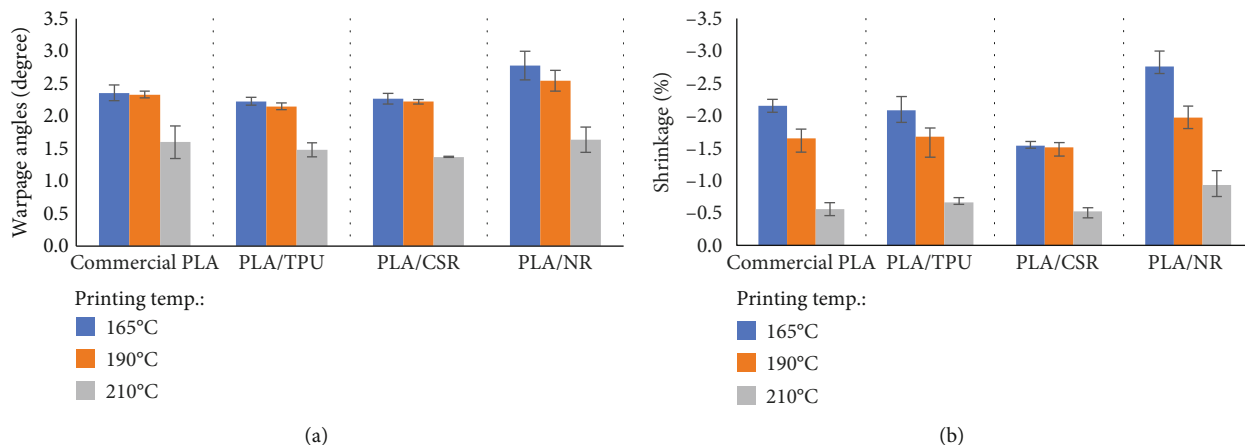


FIGURE 3: (a) The warpage angles and (b) the % shrinkage of all 3D-printed specimens at printing temperatures of 165°C, 190°C, and 210°C.

(2) *Preparation of 3D-Printed Specimens.* The obtained filaments in Section 2.2.3 and commercial PLA filament were printed into dumbbell-shaped specimens by using a ME 3D printer (Finder 2.0, Zhejiang Flashforge 3D Technology Co., Ltd) with a fan cooling at the nozzle head. The specimen size conformed with the ASTM D368 type IV standard. The printed specimens were fabricated with a hexagon pattern and 100% infill. The specimens were printed on an unheated bed with a first layer height of 0.21 mm and the latter layer height of 0.14 mm. The printing temperatures varied at 165°C, 190°C, and 210°C. The printing and travel speeds were set as 50 mm/s and 60 mm/s, respectively.

2.2.5. *Morphological Study.* The surfaces of a filament and 3D-printed specimens were observed using a digital microscope (Dino-Lite Premier AM-3013 T) at 50x and 210x magnifications. The morphologies of the filament cross-sections and the 3D-printed specimens were investigated by the Hitachi (S-3400 N Type II) Scanning Electron Microscope (SEM) operated at 15 kV and magnifications of 100x and 3000x. For the preparation of SEM specimens, the filaments and the 3D-printed specimens were immersed in liquid nitrogen for 15 min and 6 hours, respectively, before being immediately fractured and coated with gold for 200 sec.

2.2.6. *Melt Flow Index (MFI) Testing.* Melt flow indexes (MFI) of the PLA and PLA/rubber blends were tested according to the ASTM D1238-13 (Procedure A), using a melt flow indexer (GOTECH Testing Machines Inc., Taiwan). The PLA and all blends were tested at 190°C with a 2.16 kg load. The units of measure are grams of material/10 minutes (g/10 min).

2.2.7. *Thermal Analysis.* Differential scanning calorimetry (DSC) analysis was performed using The TA Instruments Discovery DSC250 to determine the thermal properties of the samples. For the first and the second heating scans, the samples were first heated from 25°C to 250°C with a heating rate of 10°C/min and kept isothermal for 2 min. For the cooling step, the samples were cooled from 250°C to 25°C also at a rate of 10°C/min. The percentage of crystallinity

of PLA in the blends was calculated using the melting enthalpy of 100% crystalline PLA (93.7 J/kg) [30].

2.2.8. *Surface Roughness Measurement.* The surface roughness of the 3D-printed specimens was measured using a Mitutoyo Surftest SJ-410 tester. The average surface index or Ra values were also calculated from the measured readings of conventional stylus-probe of surface roughness instrument, where the stylus speed was 0.5 mm/s.

2.2.9. *Tensile Measurement.* The tensile properties were determined according to ASTM D638 type IV standard using a universal tensile testing machine (Narin Instrument Co., Ltd., Thailand) with a load cell of 3 kN. The distance between the grips was 65 mm, and the crosshead speed was 5 mm/min. At least three test samples were tested for each sample, and the average values were presented. The tensile toughness in J/m^3 was calculated as the area under the stress-strain curve following the equation:

$$\text{Toughness} \left[\frac{MJ}{m^3} \right] = \int_0^{\epsilon_f} \sigma d\epsilon, \quad (1)$$

where σ is the stress in MPa, while ϵ and ϵ_f are strain and final strain at break, respectively.

3. Results and Discussion

3.1. *The Effect of Extrusion Conditions on Filament Morphologies.* The 3D printing filaments in this study were produced using a twin-screw extruder. The appropriate die head temperature for all compounds was determined to be 190°C. The morphologies of the filaments produced from PLA/rubber blends at various screw speeds and the MFI of commercial PLA, and the PLA/rubber blends are summarized in Table 1 and Figure 1, respectively. The filament sizes of all blends became larger at higher screw speeds due to a stronger die swell effect. It is worth nothing that the PLA/NR blend required the highest screw speed of 90 rpm to achieve the filament diameter above 1.75 mm, potentially due to its higher MFI (lower viscosity), leading to a lower degree of die swell. However, at screw speeds of 70 rpm

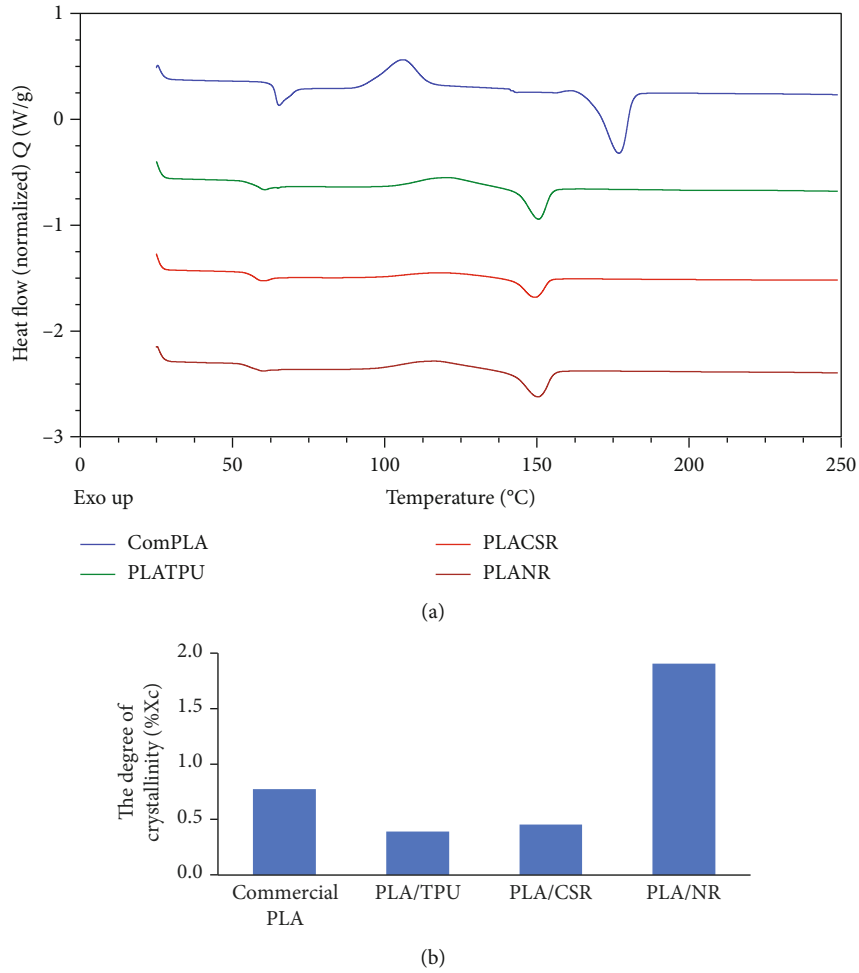


FIGURE 4: The DSC thermograms (1st heating) (a) and the degree of crystallinity (b) of PLA and the blends of PLA with different rubbers.

and above, the PLA/NR filaments were rougher, with higher fluctuation in the filament diameters. This could be explained by the shear-induced aggregation of NR particles, as observed in the SEM micrograph in Table 1(a). This effect could happen in incompatible blends under high shear [31]. On the other hand, SEM micrographs of PLA/TPU (Table 1(b)) and PLA/CSR (Table 1(c)) revealed the characteristics of compatible blends, where the rubber sizes were smaller than those of NR and were well-dispersed in PLA matrices at all screw speeds. Consequently, this led to smoother filament surfaces and lower diameter fluctuation. Moreover, these blends required a lower screw speed (70 rpm) than that for PLA/NR (90 rpm) to obtain filament diameters above 1.75 mm.

3.2. The Effect of Printing Temperature on the Specimen Properties. For the 3D printing step, the effects of printing temperature on the shape stability, surface morphology, and surface roughness of 3D-printed specimens were studied at 165°C, 190°C, and 210°C for all filaments. In this work, the shape stability was measured as a warpage angle and dimensional accuracy in the width direction of the 3D-printed specimen, where the warpage angle was measured

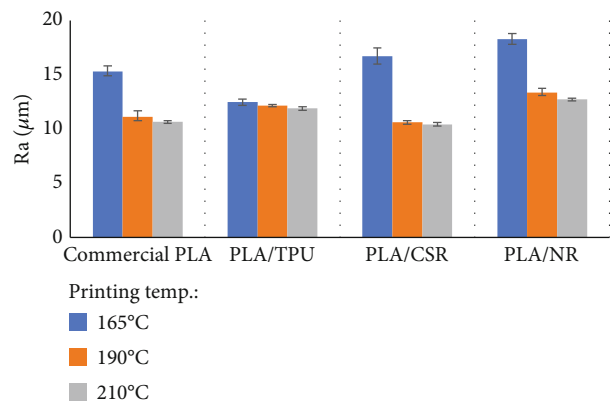
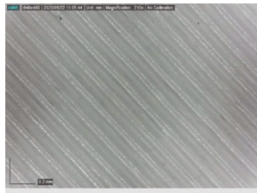
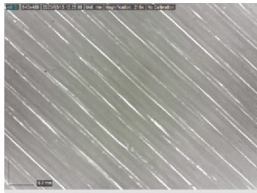
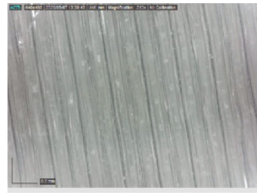
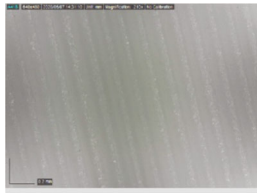

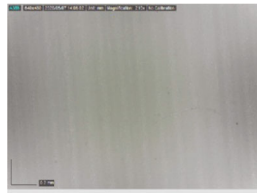
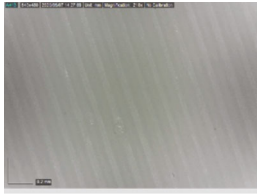
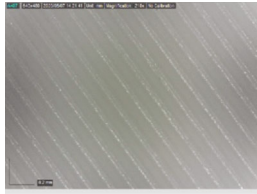
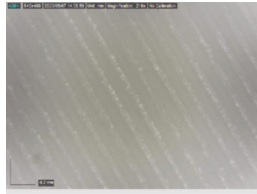
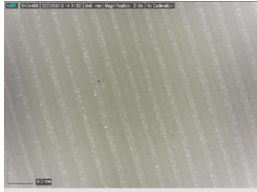
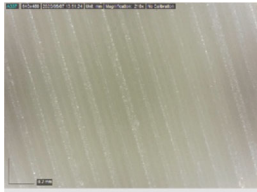
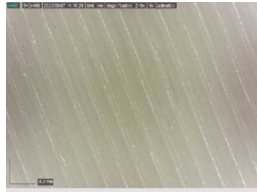


FIGURE 5: The average surface roughness (Ra value) of all 3D-printed specimens at various printing temperatures.

as described in Figure 2. The warpage angle and dimensional discrepancy (shrinkage) of all specimens are summarized in Figure 3. As can be seen, the warpage angle and shrinkage of all samples reduced when increasing the printing temperature due to the lower difference between the temperatures of the top and bottom layers. When comparing between different PLA/rubber blends, PLA/NR provided the highest

TABLE 2: Surfaces of all 3D-printed specimens produced from PLA and PLA/rubber filaments at various printing temperatures.

| Specimen | Surfaces of 3D-printed specimens at various printing temperatures (210x magnification) | | |
|----------------|--|---|--|
| | 165°C | 190°C | 210°C |
| Commercial PLA |  |  |  |
| PLA/TPU |  |  |  |
| PLA/CSR |  |  |  |
| PLA/NR |  |  |  |

warping angle and shrinkage indicating the poorest shape stability due to its highest percent crystallinity ($%X_c$) as shown in Figure 4, while PLA/CSR and PLA/TPU specimens possessed the lowest warpage angles, which were even lower than that of commercial PLA consistent with their lower $%X_c$.

The surface roughness of the specimens was measured as the average surface index or Ra values (Figure 5) and observed from the sharpness of streaks that appeared on the surface (Table 2). As can be seen, the highest printing temperature (210°C) provided the smoothest surface due to lower viscosity, which led to faster flow and better layer infusion. The surfaces were significantly rougher at the lowest printing temperature of 165°C, except for PLA/TPU, which possessed smooth surface at all printing temperatures. When comparing between different PLA/rubber blends, PLA/NR filaments provided the roughest surface when printing at 165°C, while their surface roughness was comparable at higher printing temperatures.

The effect of rubbers and printing temperature on mechanical properties of dumbbell-shaped specimens printed at 190°C and 210°C is shown in Figure 6. As can be seen, the additions of CSR and NR could increase the toughness of PLA, while the toughness of PLA blended with TPU could not change significantly. On the other hand, the

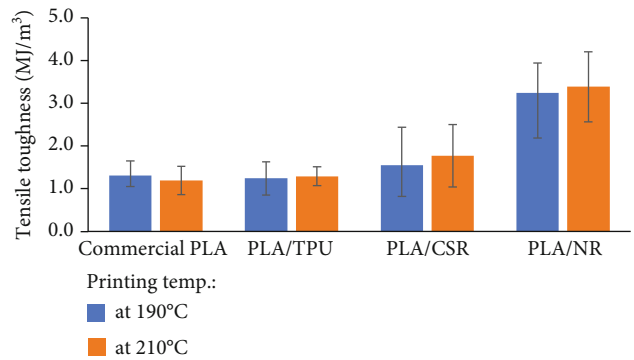


FIGURE 6: Tensile toughness of all specimens at the printing temperatures of 190°C and 210°C.

toughness of specimens produced from PLA/rubber filaments increased slightly at the higher printing temperature. This is because the presence of low- T_g rubbers in PLA led to better adhesion between printed layers at higher temperature as indicated by the SEM micrographs in Table 3.

When comparing the effect of forming techniques, the stress-strain curves of specimens fabricated by 3D printing were compared to those fabricated by compression molding

TABLE 3: The freeze-fracture surfaces of 3D-printed layer cross-sections produced from the PLA/NR filament at 100x magnification.

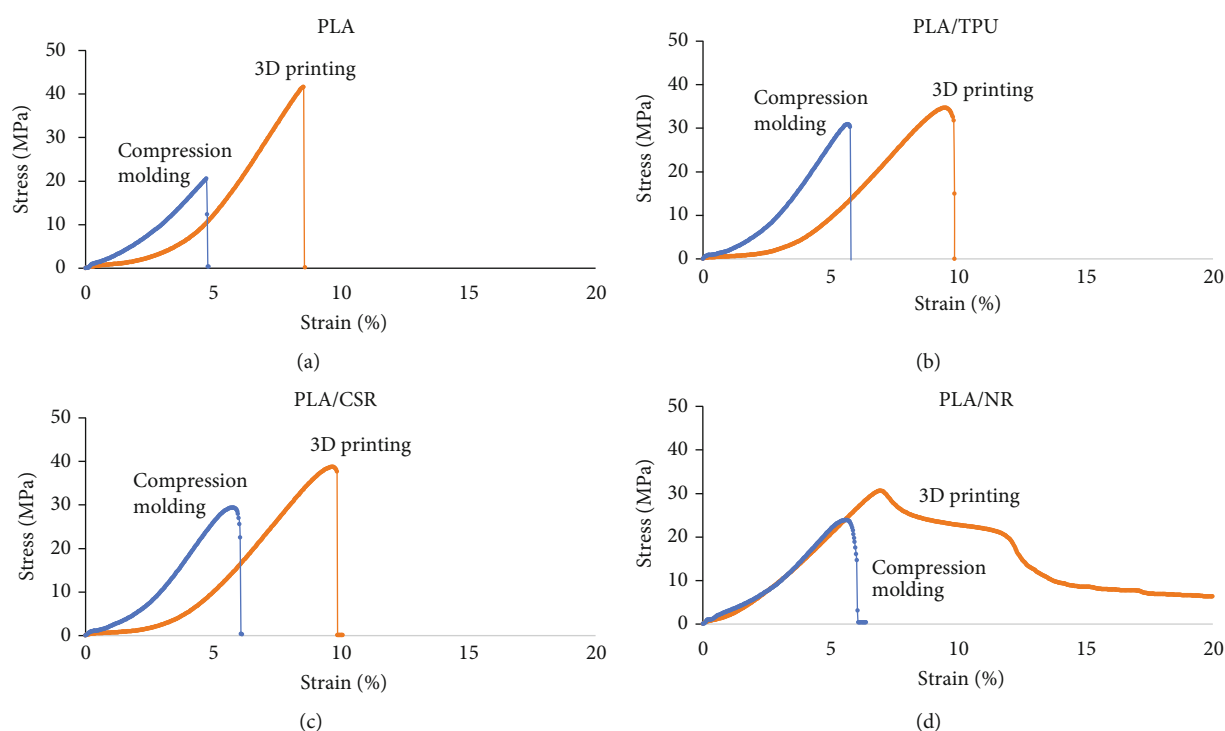
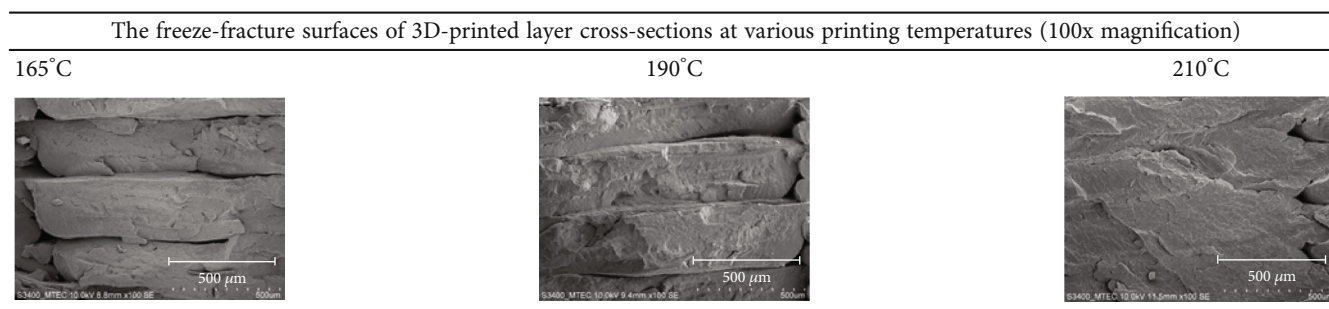


FIGURE 7: The comparison of stress-strain curves between compression-molded specimens and 3D-printed specimens fabricated from (a) PLA, (b) PLA/TPU, (c) PLA/CSR, and (d) PLA/NR at 190°C.

as shown in Figure 7. Their tensile strength, tensile toughness, and elongation at break are summarized in Figure 8. As can be seen, the shapes of stress-strain curves of samples fabricated by 3D printing and compression molding were similar for all formulations. Nevertheless, the 3D-printed specimens processed higher tensile strength, elongation at break, and tensile toughness. Interestingly, while most specimens produced by 3D printing could be stretched by almost twice as much as those produced by compression molding, the 3D-printed PLA/NR specimens could be stretched by almost 7 times more. This is probably due to the outstanding tensile strength of NR. However, it should be noted that further stretching of the 3D-printed PLA/NR specimen beyond twice the elongation of compression molded one resulted in fibrillation of the PLA/NR printed layers as shown in Figure 9(a). This could be explained by the ability of the 3D printing technique to produce specimens that aligned

in the printing direction in a fiber-like pattern, while this phenomenon was not found in the compression-molded specimens (Figure 9(b)). Note that necking was not clearly observed in our heterogeneous systems as the stretching occurred predominantly in the dispersed rubber phase.

4. Conclusion

In this work, the PLA was blended with various types of rubber (TPU, CSR, and NR) and extruded into 3D printing filaments, and the results are concluded as follows:

- (i) It was found that PLA/NR required higher screw speed (90 rpm) than PLA/TPU and PLA/CSR (70 rpm) to obtain the appropriate filament diameter in the range of 1.7–1.9 mm

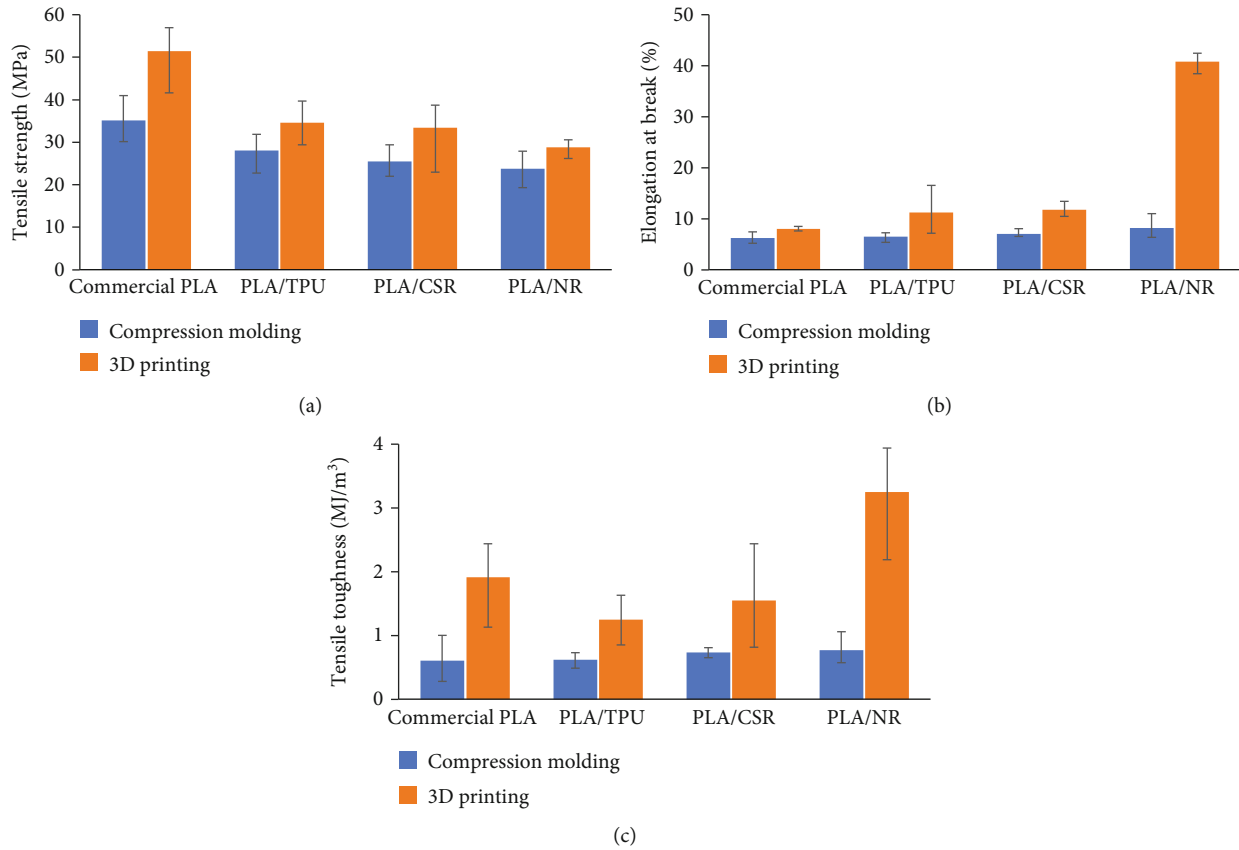


FIGURE 8: The average values of (a) tensile strength, (b) elongation at break, and (c) tensile toughness of all specimens produced by compression molding and 3D printing at 190°C.

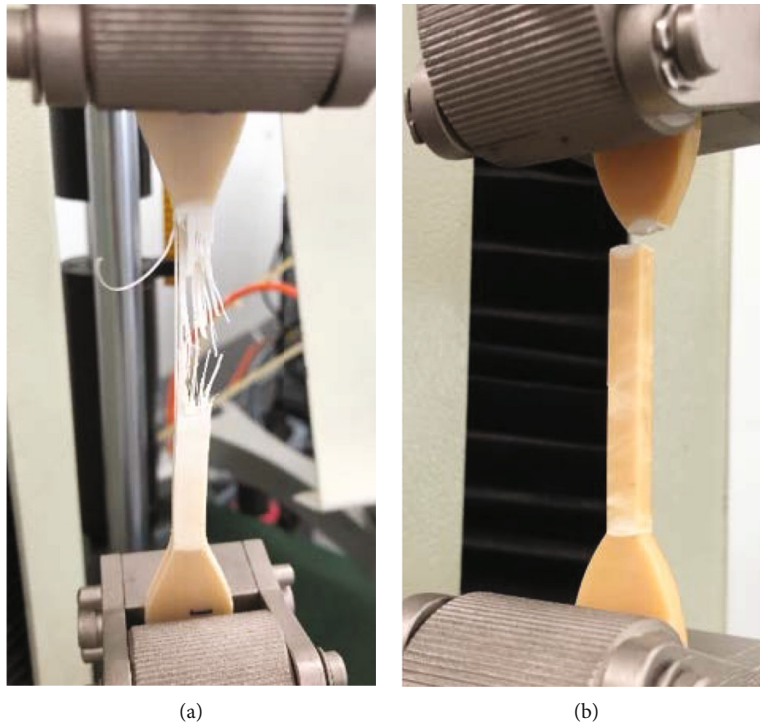


FIGURE 9: The deformation at break points of PLA/NR specimens fabricated by (a) 3D printing and (b) compression molding techniques at 190°C.

- (ii) The PLA/NR 3D-printed specimens possessed the highest tensile toughness among all. The recommended printing temperature is 210°C to obtain better shape stability
- (iii) PLA/CSR and PLA/TPU filaments could not provide higher toughness than the commercial PLA filament
- (iv) The PLA/CSR specimens possessed the best shape stability and the smoothest surface (at higher printing temperatures), while PLA/TPU could provide smooth surface even at the lowest printing temperature (165°C)
- (v) 3D printing technique could provide higher tensile toughness, tensile strength, and elongation at break than compression molding
- (vi) These PLA/rubber filaments have a good potential for producing specimens with good shape stability, surface smoothness, and high tensile toughness, especially at the printing temperature of 210°C
- (vii) The performance of these PLA/rubber filaments could be further enhanced by improving on phase compatibility and thermal stability of the blend formulations

Data Availability

The data could be requested by emailing the corresponding author.

Conflicts of Interest

The authors declare that they have no conflicts of interest.

Acknowledgments

The authors gratefully acknowledge the Ph.D. Scholarship from the Faculty of Engineering, and partial funding from the Research Unit in Polymer Rheology and Processing, Thammasat University.

References

- [1] M. Van den Eynde and P. Van Puyvelde, *3D Printing of Polylactic Acid. Industrial Applications of Poly (Lactic Acid)*, Springer, Switzerland, 2017.
- [2] D. Martinez, M. Espino, C. Honelly Mae, J. Crisostomo, and J. Dizon, "A comprehensive review on the application of 3D printing in the aerospace industry," *Key Engineering Materials*, vol. 913, pp. 27–34, 2022.
- [3] N. Shahrubudin, L. T. Chuan, and R. Ramlan, "An overview on 3D printing technology: technological, materials, and applications," *Procedia Manufacturing*, vol. 35, pp. 1286–1296, 2019.
- [4] B. Redwood, F. Schöffner, and B. Garret, *The 3D Printing Handbook: Technologies, Design and Applications*, 3D Hubs B.V., 2017.
- [5] M. Leary, *Chapter 8- Material Extrusion, Design for Additive Manufacturing*, Elsevier, 2020.
- [6] P. Angelopoulos, G. Kenanakis, Z. Viskadourakis et al., "Manufacturing of ABS/expanded perlite filament for 3D printing of lightweight components through fused deposition modeling," *Materials Today: Proceedings*, vol. 54, no. 1, pp. 14–21, 2022.
- [7] R. Singh, S. Singh, and K. Mankotia, "Development of ABS based wire as feedstock filament of FDM for industrial applications," *Rapid Prototyping Journal*, vol. 22, no. 2, pp. 300–310, 2016.
- [8] Y. Geng, H. He, H. Liu, and H. Jing, "Preparation of polycarbonate/poly(lactic acid) with improved printability and processability for fused deposition modeling," *Polymers for Advanced Technologies*, vol. 31, no. 11, pp. 2848–2862, 2020.
- [9] O. Kaynan, A. Yildiz, Y. Bozkurt, E. Ozden-Yenigun, and H. Cebeci, "Development of multifunctional CNTs reinforced PEI filaments for fused deposition modeling," in *Conference: AIAA Scitech 2019 Forum*, p. 0406, San Diego, California, 2019.
- [10] T. Tuan Rahim, A. Abdullah, H. Md Akil, D. Mohamad, and Z. Rajion, "Preparation and characterization of a newly developed polyamide composite utilising an affordable 3D printer," *Journal of Reinforced Plastics and Composites*, vol. 34, no. 19, pp. 1628–1638, 2015.
- [11] M. Zerankeshi, S. Sayedain, M. Tavangarifard, and R. Alizadeh, "Developing a novel technique for the fabrication of PLA-graphite composite filaments using FDM 3D printing process," *Ceramics International*, vol. 48, no. 21, pp. 31850–31858, 2022.
- [12] A. Plymill, R. Minneci, D. Alexander Greeley, J. Gritton, D. Alexander, and D. Greeley, *Graphene and carbon nanotube PLA composite feedstock development for fused deposition modeling*, Chancellor's Honors Program Projects, 2016.
- [13] S. Kumar, R. Singh, T. Singh, and A. Batish, "On investigation of rheological, mechanical and morphological characteristics of waste polymer-based feedstock filament for 3D printing applications," *Journal of Thermoplastic Composite Materials*, vol. 34, no. 7, pp. 902–928, 2021.
- [14] D. Fico, D. Rizzo, R. Casciaro, and C. Esposito Corcione, "A review of polymer-based materials for fused filament fabrication (FFF): focus on sustainability and recycled materials," *Polymers*, vol. 14, no. 3, p. 465, 2022.
- [15] T. M. Joseph, A. Kallingal, A. Suresh et al., "3D printing of polylactic acid: recent advances and opportunities," *International Journal of Advanced Manufacturing Technology*, vol. 125, no. 3-4, pp. 1015–1035, 2023.
- [16] B. Gupta, N. Revagade, and J. G. Hilborn, "Poly(lactic acid) fiber: an overview," *Progress in Polymer Science*, vol. 32, no. 4, pp. 455–482, 2007.
- [17] M. Singhvi, S. Zinjarde, and D. V. Gokhale, "Polylactic acid: synthesis and biomedical applications," *Journal of Applied Microbiology*, vol. 127, no. 6, pp. 1612–1626, 2019.
- [18] A. Dey, I. N. Roan Eagle, and N. Yodo, "A review on filament materials for fused filament fabrication," *Journal of Manufacturing and Materials Processing*, vol. 5, no. 3, p. 69, 2021.
- [19] S. Kumar, R. Singh, T. Singh, and A. Batish, "Comparison of mechanical and morphological properties of 3-D printed functional prototypes: multi and hybrid blended thermoplastic matrix," *Journal of Thermoplastic Composite Materials*, vol. 35, no. 5, pp. 692–707, 2022.

- [20] S. Kumar, R. Singh, T. Singh, and A. Batish, "Investigations for magnetic properties of PLA-PVC-Fe₃O₄-wood dust blend for self-assembly applications," *Journal of Thermoplastic Composite Materials*, vol. 34, no. 7, pp. 929–951, 2021.
- [21] S. Kumar, R. Singh, T. Singh, and A. Batish, "Investigations of polylactic acid reinforced composite feedstock filaments for multimaterial three-dimensional printing applications," *Proceedings of the Institution of Mechanical Engineers, Part C: Journal of Mechanical Engineering Science*, vol. 233, no. 17, pp. 5953–5965, 2019.
- [22] S. Kumar, R. Singh, T. Singh, and A. Batish, "Multimaterial printing and characterization for mechanical and surface properties of functionally graded prototype," *Proceedings of the Institution of Mechanical Engineers, Part C: Journal of Mechanical Engineering Science*, vol. 233, no. 19-20, pp. 6741–6753, 2019.
- [23] S. Kumar, R. Singh, T. Singh, and A. Batish, "Flexural, pull-out, and fractured surface characterization for multi-material 3D printed functionally graded prototype," *Journal of Composite Materials*, vol. 54, no. 16, pp. 2087–2099, 2020.
- [24] Q. Ou-Yang, B. Guo, and J. Xu, "Preparation and characterization of poly(butylene succinate)/polylactide blends for fused deposition modeling 3D printing," *Journal of the American Chemical Society*, vol. 3, no. 10, pp. 14309–14317, 2018.
- [25] W. Prasong, P. Muanchan, A. Ishigami, S. Thumsorn, T. Kurose, and H. Ito, "Properties of 3D printable poly(lactic acid)/poly(butylene adipate-co-terephthalate) blends and nano talc composites," *Journal of Nanomaterials*, vol. 2020, Article ID 8040517, 16 pages, 2020.
- [26] J. Slapnik, R. Bobovnik, M. Mešl, and S. Bolka, "Modified polylactide filaments for 3D printing with improved mechanical properties," *Contemporary Materials*, vol. 2, pp. 142–150, 2016.
- [27] I. Fekete, F. Ronkay, and L. Lendvai, "Highly toughened blends of poly(lactic acid) (PLA) and natural rubber (NR) for FDM-based 3D printing applications: the effect of composition and infill pattern," *Polymer Testing*, vol. 99, p. 107205, 2021.
- [28] S. Phattarateera and C. Pattamaprom, "Comparative performance of functional rubbers on toughness and thermal property improvement of polylactic acid," *Materials Today Communications*, vol. 19, pp. 374–382, 2019.
- [29] S. Phattarateera and C. Pattamaprom, "The Viscosity Effect of Masticated Natural Vs. Synthetic Isoprene Rubber on Toughening of Polylactic Acid," *International Journal of Polymer Science*, vol. 2019, Article ID 5679871, 9 pages, 2019.
- [30] S. Jia, D. Yu, Y. Zhu, Z. Wang, L. Chen, and L. Fu, "Morphology, Crystallization and Thermal Behaviors of PLA-Based Composites: Wonderful Effects of Hybrid GO/PEG via Dynamic Impregnating," *Polymers*, vol. 9, no. 12, p. 528, 2017.
- [31] J. S. Hong, Y. K. Kim, K. H. Ahn, and S. Lee, "Shear-induced migration of nanoclay during morphology evolution of PBT/PS blend," *Journal of Applied Polymer Science*, vol. 108, no. 1, pp. 565–575, 2008.